

# Energy transfer and charge separation kinetics in photosystem I

## Part 1: Picosecond transient absorption and fluorescence study of cyanobacterial photosystem I particles

Alfred R. Holzwarth,\* Günther Schatz, Helmuth Brock, and Edith Bittersmann

Max-Planck-Institut für Strahlenchemie, D-4330 Mülheim an der Ruhr, Germany

**ABSTRACT** The energy transfer and charge separation kinetics of a photosystem I (PS I) core particle of an antenna size of 100 chlorophyll/P700 has been studied by combined fluorescence and transient absorption kinetics with picosecond resolution. This is the first combined picosecond study of transient absorption and fluorescence carried out on a PS I particle and the results are consistent with each other. The data were analyzed by both global lifetime and global target analysis procedures. In fluorescence major lifetime components were found to be 12 and 36 ps. The shorter-lived one shows a negative amplitude at long wavelengths and is attributed to an energy transfer process between pigments in the main antenna Chl pool and a small long-wavelength Chl pool emitting around 720 nm whereas the longer-lived component is assigned to the overall charge separation lifetime. The lifetimes resolved in transient absorption are 7–8 ps, 33 ps, and  $\geq 1$  ns. The shortest-lived one is assigned to energy transfer between the same pigment pools as observed also in fluorescence kinetics, the middle component of 33 ps to the overall charge separation, and the long-lived component to the lifetime of the oxidized primary donor P700<sup>+</sup>. The transient absorption data indicate an even faster, but kinetically unresolved energy transfer component in the main Chl pool with a lifetime <3 ps. Several kinetic models were tested on both the fluorescence and the picosecond absorption data by global target analysis procedures. A model where the long-wave pigments are spatially and kinetically connected with the reaction center P700 is favored over a model where P700 is connected more closely with the main Chl pool. Our data show that the charge separation kinetics in these PS I particles is essentially trap limited. The relevance of our data with respect to other time-resolved studies on PS I core particles is discussed, in particular with respect to the nature and function of the long-wave pigments. From the transient absorption data we do not see any evidence for the occurrence of a reduced Chl primary electron acceptor, but we also can not exclude that possibility, provided that reoxidation of that acceptor should occur within a time <40 ps.

## INTRODUCTION

Photosystem (PS)<sup>I</sup> is the photosystem of oxygenic photosynthesis that receives electrons from PS II via the mobile plastoquinone pool and reduces NADP<sup>+</sup> to NADPH (see reference 2 for a general review on biochemistry and structure of PS I). In PS I of both cyanobacteria and higher plants the kinetics of energy migration to and charge separation in the reaction center is only scarcely understood so far. Of particular interest is the question whether the overall exciton decay kinetics in PS I antenna is trap limited (by charge separation) as found for PS II (for review see reference 3) or limited by exciton diffusion in the antenna (4–6). An answer to this question requires a detailed understanding of the energy migration kinetics between the various chlorophyll (Chl) antenna forms. It is now promising to study the energy transfer kinetics by various ultrafast spectroscopic techniques to address these questions (for recent reviews see references 3, 4, 7, 8). In addition, however, the understanding of these processes would greatly benefit from a detailed knowledge about the antenna struc-

tures, which is still not at hand. There is reason to hope, however, that such information will soon become available for some Chl antenna structures (9–11). It is generally believed that all PS I core antenna of both higher plants and cyanobacteria are basically identical. For cyanobacteria all Chl pigments in PS I are located in the core antenna with an antenna size of  $\sim 100$  Chl/P700. Higher plants and green algae contain in addition several Chl b containing polypeptides that are bound to the core as peripheral antenna complexes (2). The bulk of the PS I Chl a core antenna absorbs at 675–678 nm and generally emits with a maximum around 684 nm and sometimes up to 695 nm at room temperature (often referred to as F690) (12).

The antenna of PS I in higher plants, green algae, and cyanobacteria is spectrally heterogeneous, containing various chlorophyll pigments each with characteristic absorbance and corresponding fluorescence spectra (13, 14). This spectral heterogeneity can be understood as an inhomogeneous spectral broadening of the Chl spectra by varying site interactions with the surrounding protein (15, 16). In addition to general line broadening a special red-shifted (as compared with the main absorption peak) pigment called C695 has been held responsible for the low and room temperature fluorescence emission band (F720) whereas the pigment C705 has been attributed to the low temperature emission band at about 735 nm (F735) (17). The function of these long wavelength pigments, absorbing at wavelengths longer than the reac-

A preliminary account of this work was presented at the VIIIth International Congress on Photosynthesis, Stockholm, 1989 (1).

\* Address correspondence to Alfred R. Holzwarth.

<sup>1</sup> Abbreviations used in this paper: Chl, chlorophyll; DADS, decay-associated difference (absorption) spectrum; DAS, decay-associated spectrum; EPR, electron paramagnetic resonance; P700, reaction center of photosystem I; PMS, phenazine metho-sulfate; PS, photosystem; RC, reaction center; SADS, species-associated difference (absorption) spectrum; SAS, species-associated spectra.

tion center (RC), in PS I and other photosystems is not clear at present. Several authors have suggested that they should serve to concentrate energy near the RC to make charge separation faster and thus more efficient (18, 19).

The time dependence of the fluorescence and transient absorption from the various spectral Chl forms should provide a handle that enables one to follow directly the energy migration between them. In combination with advanced data analysis methods (20–22) and kinetic modelling (23–25) this could eventually lead to a detailed structural and kinetic description of the antenna and RC. In principle it should be possible to excite the various spectral Chl forms more or less selectively. In that case we may expect fast kinetic terms that reflect the equilibration processes in the antenna. In the kinetics of those forms that were not excited directly, but obtain excitation density via energy transfer processes, we may expect rise terms (negative amplitude kinetics) provided that the time resolution of the experiment is sufficient (26). Such rise kinetics, in some cases even of biexponential nature, have been observed previously only at low temperatures in the fluorescence of PS I by various groups with time constants of up to 140 ps (18, 27, 28). At room temperature rise terms, being directly indicative of energy transfer between various spectral forms, were generally not observed, neither for particles of small antenna size (6, 29) nor for the larger PS I particles (18). So far the only known cases with resolved rise kinetics at room temperature are the PS I core particles from the blue-green alga *Synechococcus sp.* reported here (see also reference 1 for a preliminary report and reference 30 for a temperature-dependent fluorescence study), and a stroma-thylakoid preparation from spinach which was detergent free and had the natural antenna size of ~200 Chl/P700 (1). It is important to realize that the kinetic and spectral properties of these fast processes have a great diagnostic potential for elucidating the detailed energetics and structure/function relationships of antenna complexes in general and of PS I antenna in particular (3, 8, 23).

A nearly diffusion-limited exciton kinetics of PS I complexes has been suggested in the past on the basis of data from a study of particles of various antenna sizes (6). In contrast, from a detailed study on isolated PS II particles we concluded that in PS II the charge separation was trap-limited (31). For PS I this question has to be answered independently in view of the fact that the antenna structure for PS I is quite different from PS II and that P700 is a deeper trap than P680 in PS II with respect to the energy of the surrounding antenna Chls. Several groups have studied the PS I kinetics by time-resolved fluorescence (1, 12, 14, 18, 29, 30, 32–35) and transient absorption kinetics (36–40). Despite this substantial amount of work no agreement has been reached so far on the interpretation of the basic processes in the antenna and RC.

In this contribution we report on a combined picosecond fluorescence and transient absorption study of the energy transfer and charge separation kinetics in PS I particles isolated from the thermophilic cyanobacterium *Synechococcus sp.* Studying the kinetics of these PS I particles is particularly interesting in view of the fact that their steady state room temperature emission maximum is located around 720 nm, i.e., at longer wavelength than for other reported PS I preparations, except for what was believed to be a native PS I preparation from spinach, which also had a long-wavelength maximum (18). The present preparation might thus be amenable to elucidate more clearly the energy migration in the antenna between the various spectral forms, and in particular the long wavelength absorbing forms, than has been possible previously. This work has several objectives: first, the combined transient absorption and fluorescence kinetic study should potentially provide for a more detailed picture of the antenna equilibration and charge separation processes than each method alone. Second, we present a detailed absorption spectral analysis that allows us to predict both fluorescence spectra and lifetimes assuming that thermal equilibrium is established. Third, we want to address the problem as to the nature of the primary electron acceptor  $A_0$  in PS I. Several reports have appeared in the literature pointing to a monomeric Chl a pigment that should serve this function (41–43). However, a substantial part of the evidence for that intermediate came from electron paramagnetic resonance (EPR) or optical studies at low temperatures, which might not reflect properly the processes at physiological temperature (42, 44–46). At the same time, the evidence that has appeared from transient absorption studies at higher temperatures in favor of  $A_0$  being a Chl molecule is only indirect, i.e., it was seen clearly only with reduced secondary acceptors (43) whereas the difference spectrum attributed to  $\text{Chl}^-$  when secondary acceptors were oxidized was quite unusual in shape (47).

## MATERIALS AND METHODS

Thylakoid membranes from the thermophilic cyanobacterium *Synechococcus sp.* were obtained according to reference 48. PS I particles were isolated from thylakoids by extraction with Triton X-100 and subsequent sucrose density gradient centrifugation (48). This preparation is highly homogeneous and contains only negligible amounts of functionally uncoupled Chls, which has been a problem with other preparations in the past. The Chl a/P700 ratio is  $\sim 100 \pm 10:1$  as determined by the method described in reference 49. Unless stated otherwise all samples contained ascorbate (3 mM) and phenazine metho-sulfate (PMS) (20  $\mu\text{M}$ ) during measurements. For fluorescence measurements the particles were diluted with Tris buffer (containing 0.05% Triton X-100) to a Chl concentration of 8–10  $\mu\text{g}/\text{ml}$ . Absorption spectra were measured on a spectrophotometer (model PE 320; Perkin-Elmer Cetus Instruments, Norwalk, CT). Corrected steady state emission and excitation spectra were measured on a Spex-Fluorolog instrument (SPEX Industries Inc., Edison, NJ) (50).

Picosecond fluorescence kinetics were measured by the single-photon counting technique with 5 ps resolution using a micro-channel-

plate detector (model 1564U-01, Hamamatsu Corp., Bridgewater, NJ). Excitation occurred at 670 nm with picosecond pulses of very low intensity at a repetition rate of 400 kHz. The apparatus response was <50 ps (FWHM). Fluorescence was resolved by a double monochromator (model DH10, Jobin Yvon, Longjumeau, France) with 4-nm resolution. The fluorescence lifetime measurements were carried out under magic angle polarization conditions to avoid interference with anisotropy decay components. The sample was pumped through a flow measuring cuvette ( $1.5 \times 1.5 \times 1.5$  mm<sup>3</sup>), thermostatted at 5°C at a flow rate of ~100 ml/min. Fluorescence decay data were analyzed as a sum of exponentials by using the global analysis procedure as described (51). The data are presented as decay-associated fluorescence spectra (DAS), which is a plot of the amplitude of a component versus emission wavelength (20). The DAS were calculated from each set of decays recorded over the whole emission wavelength range. The amplitudes of the DAS were corrected for the wavelength dependence in the sensitivity of the detector and the measuring time at each wavelength.

Picosecond transient absorption kinetics was measured by the apparatus described in reference 52 using independently tunable excitation and probe wavelengths. The cross-correlation between pump and probe pulses was  $\leq 15$  ps wide (FWHM). Excitation occurred at 678 nm, i.e., near the absorption maximum with a pulse energy of generally  $\approx 5 \mu\text{J}/\text{cm}^2$  per pulse and a repetition rate of 80 kHz. At this excitation intensity <1 out of 200 Chls was excited per pulse. Thus double excitation of a PS I complex and singlet annihilation effects can be ruled out. Reducing further the excitation intensity by up to a factor of 5 did not have any effect on the observed kinetics. The pump and the probe beams were polarized at magic angle to each other. The samples for transient absorption had an OD = 0.6–0.7/mm at the excitation wavelength. The sample cuvette had a pathlength of 1 mm and the sample was pumped at a flow speed of  $\approx 500$  cm/s. At this high sample pumping speed <10% of the sample volume received a subsequent excitation pulse. Absolute absorption differences were measured over a delay time of  $\sim 1$  ns. The data from kinetic traces at different detection wavelengths were analyzed by a similar global data analysis procedure as described above for the fluorescence decays. The fitting procedure involved deconvolution with the measured cross-correlation function. From measurements with dye molecules we verified that lifetimes down to  $\sim 2$  ps could be accurately resolved. The absorption difference  $\Delta A$  as a function of time  $t$  and detection wavelength  $\lambda_d$  is given by the sum of exponentials

$$\Delta A(t, \lambda_d) = \sum_{i=1}^n \Delta A_i(\lambda_d) \times \exp^{-t/\tau_i}, \quad (1)$$

where  $\Delta A_i(\lambda_d)$  is the decay-associated absorption difference spectrum (DADS) of lifetime component  $\tau_i$ .

Target analysis (sometimes called compartmental analysis [22, 53]) of the picosecond transient absorption and the fluorescence data was carried out similarly as described before for fluorescence kinetics (30, 54). The results of this analysis, assuming a specific kinetic model, are the set of rate constants  $k_{ij}$  for energy transfer between pools of pigments (compartments) as well as the charge separation rate constant(s). Furthermore the species-associated spectra (SAS) in fluorescence and species-associated difference spectra (SADS) in transient absorption, respectively, are obtained.

## RESULTS

The room temperature absorption and corrected fluorescence emission spectra of the *Synechococcus* PS I particles are shown in Fig. 1. The maximum of the steady state emission occurs at 718 nm (F720) while the emission exhibits a shoulder at 690 nm. The stationary fluorescence (Fig. 1 B) shows a large apparent Stokes shift.

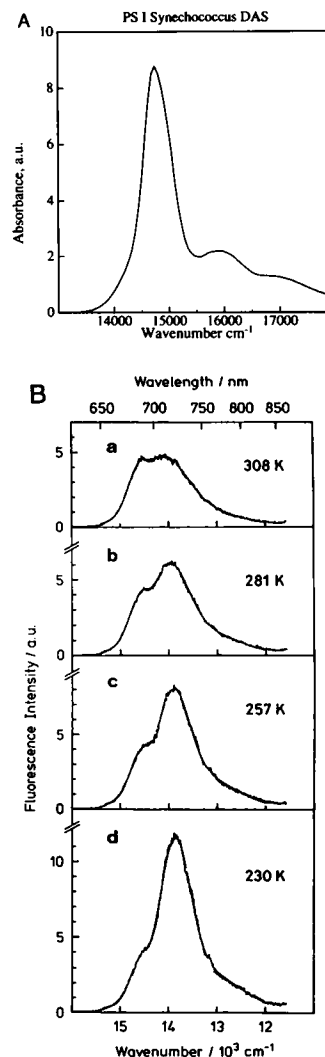


FIGURE 1 Steady state absorption (full line) of PS I particles from *Synechococcus* at room temperature (A) and (B) temperature dependence of corrected fluorescence emission spectra of PS I particles from *Synechococcus*.  $\lambda_{\text{exc}} = 650$  nm.

Judging from the absorption maximum, which is located at 678 nm, the main emission (F720) occurs from a small long-wavelength pigment pool containing only a few pigments whereas the bulk of the Chl pigments emits only with low intensity (F690). The latter emission is highly temperature dependent and is further decreased strongly by lowering the temperature (c.f., Fig. 1 B).

## Fluorescence kinetics

Fluorescence decays were recorded at emission intervals of 5 nm to a high S/N ratio ( $\geq 40$  000 counts in the peak) upon excitation at 670 nm, i.e., at the blue edge of the absorption maximum. Fig. 2 shows an example of fluorescence decays measured at 690 and 720 nm, respectively. The fast components are dominant whereas long-

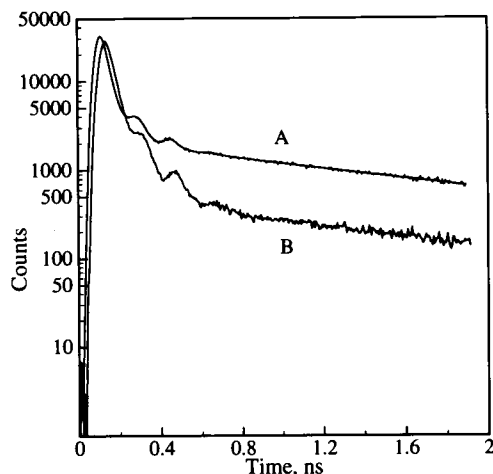


FIGURE 2 Fluorescence decays of PS I particles at 5°C.  $\lambda_{\text{exc}} = 670$  nm. (A)  $\lambda_{\text{em}} = 690$  nm; (B)  $\lambda_{\text{em}} = 720$  nm.

lived components contribute only very little to the fluorescence. Fig. 3 shows the picosecond time-resolved emission (DAS) calculated by global analysis for the PS I particles at 5°C under reducing (ascorbate) conditions. No significant change in fluorescence lifetimes nor in DAS was observed when P700 was oxidized by ferricyanide (not shown). Generally three and sometimes four exponential lifetime components were required for a good fit of the picosecond fluorescence data (c.f., Table 1). Only two of the components, the shortest-lived ones, have a substantial relative amplitude. The fastest component ( $\tau_1$ ) has a lifetime of  $12 \pm 1$  ps. It shows positive amplitude below 700 nm and negative amplitude above. The positive maximum is located at 690 nm and the negative maximum  $\sim 730$  nm. This behavior clearly indicates an energy transfer process from the F690 to the

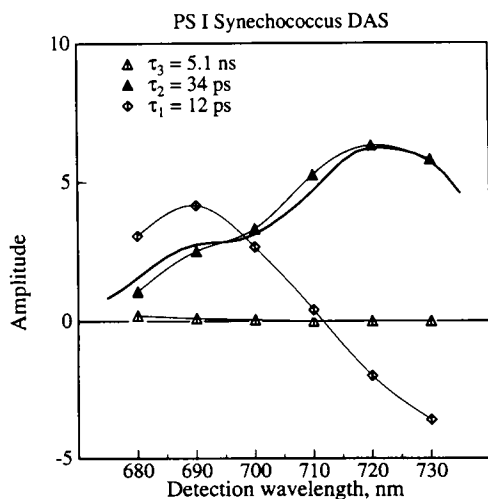


FIGURE 3 Fluorescence DAS of PS I particles at 5°C as calculated by global analysis from fluorescence decays.  $\lambda_{\text{exc}} = 670$  nm.

TABLE 1 Lifetimes and assignment of kinetic components from global analysis of fluorescence ( $T = 5^\circ\text{C}$ ) and transient absorption ( $T = 12^\circ\text{C}$ ) data on PS I particles from *Synechococcus*.  $\lambda_{\text{exc}} = 670$  nm in fluorescence;  $\lambda_{\text{exc}} = 678$  nm in transient absorption

Lifetimes	Fluorescence	Transient absorption	Assignment
<i>ps</i>			
$\tau_1$	$12 \pm 1$	$8 \pm 1$	Exciton equilibration
$\tau_2$	$35 \pm 3$	$33 \pm 3$	Charge separation
$\tau_3$	—	$>10$ ns	P700 <sup>+</sup> lifetime
$\tau_4$	1,300–1,700	—	Uncoupled Chl; small amplitude*

\* With very long ( $>5$  ns) fitting window occasionally an  $\sim 5$ -ns component with minor ( $\leq 0.1\%$ ) amplitude was seen in addition in fluorescence.

F720 emitting pigments. The second lifetime component ( $\tau_2 = 35 \pm 3$  ps) shows two bands in the corresponding DAS. The one with lower intensity is located at 690 nm (F690) whereas the intensity maximum occurs at 720 nm. In addition to these two predominant lifetime components with large amplitude we observed one or occasionally two components with very small relative amplitudes ( $<1\%$ ). Their lifetimes were in the 1.3–5 ns range. We attribute them to a small amount of uncoupled Chl since their emission spectra (DAS) have their maxima at wavelengths well below 680 nm. It is interesting to note that these long-lived contributions were found to be much smaller (always  $<1\%$  and in many preparations  $<0.2\%$ ) than observed in most previously published work on detergent-isolated PS I particles. This suggests that the PS I particles studied here are particularly pure and the Chls are well coupled to the antennae. We believe this to be a consequence of the thermophilic nature of the *Synechococcus* strain used. We should like to note that even a few percent in amplitude of these long-lived components can totally obscure and dominate the apparent fluorescence yield and thus the entire steady state emission spectrum of PS I particles. In addition long-lived fluorescence emission components with significant amplitude may cause substantial problems in data analysis of the fast components.

### Transient absorption kinetics

Transient absorption kinetics have been measured at  $12 \pm 2^\circ\text{C}$  in the wavelength range from 660 to 720 nm upon excitation at 678 nm (i.e., the absorption maximum). At the low excitation densities of typically  $5 \mu\text{J}/\text{cm}^2$  per pulse we can exclude nonlinearities due to singlet annihilation. This was confirmed by the fact that no changes in the kinetics were observed when decreasing the excitation density of the pulses by up to a factor of 5. Fig. 4 shows typical transient absorption traces for various detection wavelengths. All of these signals are

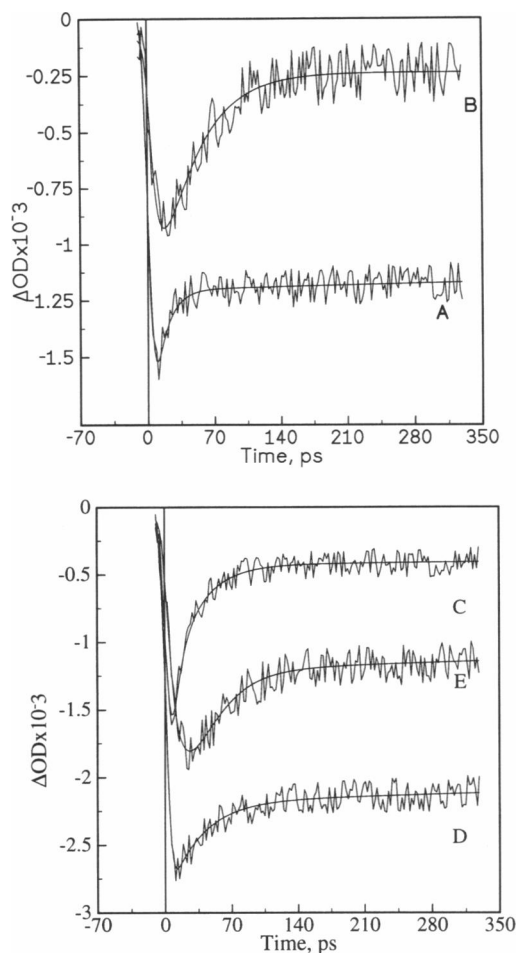


FIGURE 4 Transient absorption kinetics of PS I particles.  $\lambda_{\text{exc}} = 678$  nm. (A)  $\lambda_{\text{det}} = 680.5$  nm; (B)  $\lambda_{\text{det}} = 720.5$  nm; (C)  $\lambda_{\text{det}} = 690.5$  nm; (D)  $\lambda_{\text{det}} = 700.5$  nm; (E)  $\lambda_{\text{det}} = 711$  nm; all traces on absolute scale (for reasons of clarity only the first 300 ps are shown).

bleaching signals. Only around 660 nm some absorption increase was observed. The kinetic traces from all detection wavelengths were subjected to a global analysis procedure. Three lifetime components were necessary to describe the kinetics well over the whole detection wavelength range and a delay range of 1 ns. These lifetimes were  $\tau_1 = 7\text{--}9$  ps,  $\tau_2 = 31\text{--}35$  ps, and  $\tau_3 \gg 1$  ns (the ranges in lifetimes refer to different measurements and samples). Since our maximal delay range was only 1 ns the latter lifetime is not determined accurately. Generally values between 300 and 700 ns were obtained in the fitting procedure. This should be interpreted simply in the sense that the long-lived component decays only on a time scale much larger than the time scale of the experiment (i.e., 1 ns). The DADS of the three lifetime components are given in Fig. 5 and the lifetimes are summarized in Table 1. The  $\tau_1$  component (7–9 ps) shows a maximal bleaching near 685 nm (negative  $\Delta\text{OD}$ ) and a strong absorption increase (positive  $\Delta\text{OD}$ ) at 710 nm. The  $\tau_2$  component (31–35 ps) shows a weak bleaching

maximum at 690 nm and maximal bleaching at  $\approx 715$  nm. Below 680 nm a broad absorption increase is seen. The long-lived  $\tau_3$  component shows two bleaching maxima at 685 and 700 nm, respectively. Care should be taken in interpreting the DADS, however, since each of these kinetic components spectra represents a superposition of all spectra of the intermediate states, weighted by the corresponding kinetics (26, 31). This should not be confused with the more usual but less informative presentation of absorption difference spectra at particular times after the excitation pulse, where kinetic components are mixed to various extents (see Fig. 6 for a difference spectrum at zero delay time). A DADS, in contrast, gives information on a spectral component associated with a certain lifetime only.

Only the DADS of the  $\tau_3$  component in Fig. 5 represents the difference spectrum of a pure component, i.e., of the intermediate present at very long time after the excitation pulse ( $t \gg 1$  ns). Following the definition of the DADS (Eq. 1), the difference spectrum at time  $t = 0$  is given by the sum of the amplitudes of all decay-associated components at a particular wavelength (shown in Fig. 6,  $\Sigma_{1+2+3}$ ). This absorption difference spectrum at  $t = 0$  shows two absorption bleaching bands of comparable intensity at 685 and at 700 nm. Likewise on the basis of the definition of a DADS we can obtain the absorption difference spectrum corresponding to the fast  $\tau_1$  process alone by summing the amplitudes of components  $\tau_2$  and  $\tau_3$  at each wavelength (shown in Fig. 6,  $\Sigma_{2+3}$ ). This spectrum essentially represents the absorption difference spectrum at a time between the end of the fast  $\tau_1$  and the beginning of the slower  $\tau_2$  process. (Note that this simple procedure of getting the spectrum of a specific interme-

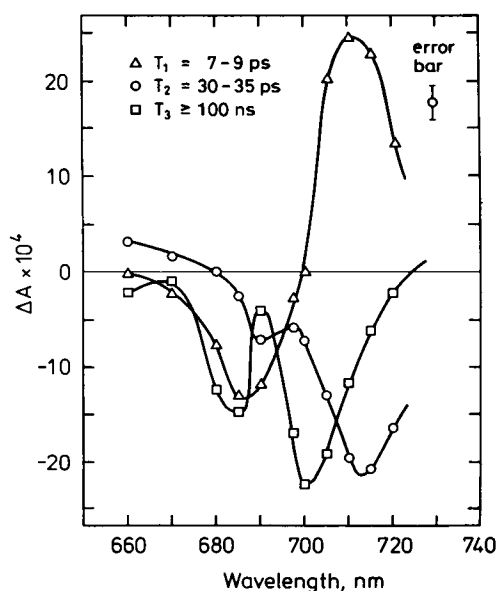


FIGURE 5 Decay-associated absorption difference spectra (DADS) of PS I particles as calculated from the absorption kinetic traces by global analysis.  $\lambda_{\text{exc}} = 678$  nm;  $T = 12^\circ\text{C}$ . P700 reduced.

TABLE 2 Optimal rate constants  $k$  [ $\text{ns}^{-1}$ ] from kinetic model 7A\* (Fig. 7 A)

Rate constant	Fluorescence	Transient absorption	Comments
$k_{12}$	8.5	16	Back energy transfer from pool 2
$k_{21}$	61	86	Forward energy transfer to pool 2
$k_{22}$	45	40	Effective charge separation

\* Maximum errors in rate constants are  $\pm 10\%$ .  
See also comment to Table 3.

diode is exact only when the differences between lifetime components are large; this is not exactly the case here [8 and 35 ps] and we thus have to accept a somewhat larger error in the resulting spectrum; an exact procedure to get species-associated spectra is given below; in view of the simplicity of the procedure we nevertheless present the result here and comparison with the exact results given below shows that this simple procedure is in fact still quite reasonable in this case). It shows absorption bleachings at 685 nm and a broad bleaching band at 705 nm with a shoulder at 715 nm.

## DISCUSSION

### Fluorescence data

Comparison of the absorption and fluorescence spectra (Fig. 1 A and B) indicates that the main emission originates from a small pool of long-wavelength-emitting pigments, which contributes only little to the absorption. As seen in Fig. 1 the main pool of pigments absorbs in the range 666–686 nm and does not fluoresce strongly. Thus the steady state emission can be interpreted in terms of a rapid equilibration of the excitons in the originally excited main pool with a small pool of Chls emitting the long-wavelength band F720. This picture is supported by the time-resolved fluorescence experiments.

TABLE 3 Rate constants  $k$  [ $\text{ns}^{-1}$ ] calculated for model C (Fig. 7 C) by target analysis from transient absorption and fluorescence kinetics data

Rate constant	Fluorescence	Transient absorption*	Comments
$k_{12}$	39	64	Energy transfer from long-wavelength pool 2 to short-wavelength pool 1
$k_{21}$	12	26	Energy transfer from short-wavelength pool 1 to long-wavelength pool 2
$k_{11}$	60	49	Charge separation

\* Rate constants  $k_{12}$  and  $k_{21}$  are higher in transient absorption because of the faster  $\tau_1$  lifetime as compared with fluorescence; rate constant  $k_{12}$  also higher because of higher temperature in transient absorption.

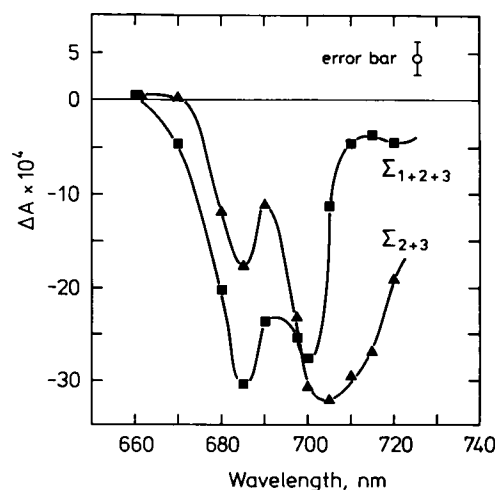


FIGURE 6 Absorption difference spectra of PS I particles at  $t = 0$  after the excitation pulse ( $\Sigma_{1+2+3}$ ) and after the completion of the fast  $\tau_1$  process ( $\Sigma_{2+3}$ ). These curves were calculated from the data in Fig. 5.

The DAS of the fluorescence  $\tau_1$  component (Fig. 3) shows a negative amplitude (rise term) in the long-wavelength range. This feature unequivocally characterizes the process as an energy transfer process ( $\tau_1 = 12$  ps), which decreases the population in the initially excited F690 emitting pool and transfers excitation to the F720 emitting pool. Correspondingly the  $\tau_2$  component in the DAS of Fig. 3 seems to reflect the overall decay of the excitons in the antenna. The most reasonable tentative interpretation of the  $\tau_2$  process is charge separation in the reaction center. This assignment is in fact confirmed by the transient absorption data presented below, which yield directly the appearance kinetics of  $P_{700}^+$ . The DAS of the  $\tau_2$  component does not show any features of energy transfer between spectrally different pools, i.e., a negative amplitude is missing. The one or sometimes two long-lived fluorescence components with very low amplitude clearly originate from functionally uncoupled Chls, as is suggested by the DAS, which peak well below 680 nm. We will therefore not discuss these components any further.

In a straightforward interpretation the simplest kinetic scheme that evolves from the steady state and kinetic fluorescence data is shown in Fig. 7 A. The temperature dependence of the fluorescence spectra (Fig. 1 B) shows that there exists a thermal equilibrium between fluorescence components at 690 nm (F690) and fluorescence at 720 nm (F720). The initially excited Chl pool 1 equilibrates with the long-wavelength Chls (F720) in a time of  $\sim 12$  ps. After this time the excitons are essentially equilibrated over the entire antenna and no longer-lived antenna equilibration processes seem to happen as can be concluded from the absence of any longer-lived kinetic components with energy transfer character. The charge separation occurs with an apparent lifetime of 35 ps from a Chl pool that appears to be more closely asso-

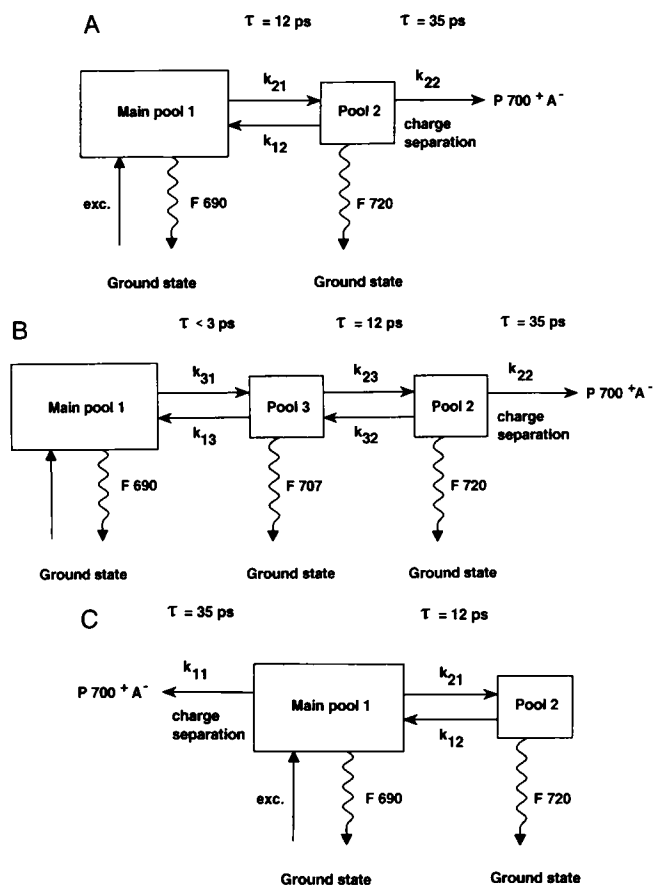


FIGURE 7 Different kinetic models for the energy transfer and charge separation processes in PS I particles. All models are discussed in detail in the text.

ciated with the long-wavelength emitting Chl pool (F720) than with the main pool of Chls (F690). Assuming this compartmental kinetic model (Fig. 7 A), we have fitted the fluorescence lifetime data and calculated the corresponding rate constants for antenna equilibration and charge separation by target analysis. The results are given in Table 2. The forward transfer rate  $k_{21}$  is very rapid compared with the back transfer rate  $k_{12}$  of excitation between pools 1 and 2. The fairly low *apparent* charge separation rate constant  $k_{22}$  from the RC indicates that the excitation is delocalized over quite a large number of antenna molecules. This is reminiscent of the situation that we have found earlier in PS II particles (31). The lifetimes and rate constants in Table 2 already indicate that the exciton kinetics is more trap limited than diffusion limited, since even the slowest energy transfer steps between Chl pools are at least a factor of three faster than the overall charge separation lifetime (see below for a more detailed discussion). Our measurements on this PS I particle present the first case where this internal equilibration component has been resolved at higher temperatures by way of the rising (negative amplitude) component at long wavelengths in both absorption and fluorescence detection (see also reference 1

and Turconi et al. (30) for a temperature study). This observation unequivocally allows us to attribute the fast component to exciton equilibration between two or more pigment pools. We have observed a similarly fast antenna equilibration component at room temperature also in one other PS I preparation, i.e., the stroma thylakoid fraction isolated from spinach chloroplasts (1) and more recently in detergent isolated PS I particles from spinach (55). We note that an ultrafast antenna equilibration kinetics in intact chloroplasts and green algae of  $\sim 15$  ps lifetime, which are attributed at least partly to PS I, recently was found by us as well (5, 56).

## Transient absorption data

The transient absorption data (Figs. 5 and 6) show contributions from both energy transfer and charge separation. The spectral and kinetic component that can be assigned most easily is the long-lived absorption difference component ( $\tau_3 > 10$  ns). This DADS shows well-known characteristic features and is essentially identical with the one measured by Nuijs et al. (47) and Il'ina et al. (57) in PS I particles from spinach or beans, respectively. It is attributed to the primary charge separation process giving rise to the absorption difference spectrum of the RC ( $P700^+ - P700$ ). This interpretation is also consistent with the fact that the transient spectrum does not decay on the time scale of our measurement. After the formation of the  $P700^+$  signal with a time constant of  $\sim 33$  ps we do not observe any slower processes on the time scale  $\leq 1$  ns. We can thus exclude any secondary electron transfer processes occurring significantly slower than  $\sim 40$  ps and giving rise to an absorption change in the 660–720 nm wavelength range. This excludes, inter alia, a slow ( $t > 40$  ps) reoxidation of a  $Chl^-$  molecule that has been suggested to function as the primary electron acceptor in PS I (47) (see below for a further discussion).

The interpretation of the other two kinetic components (DADS) is more difficult. The absorption difference at time  $t = 0$  (Fig. 6) shows two bleaching bands. In principle this spectrum should comprise the ( $Chl^* - Chl$ ) absorption difference spectrum. That difference spectrum is expected to be composed of the proper ground state absorption bleaching of the excited pigments, which should be a mirror image of the absorption, and a slightly red-shifted contribution of similar intensity and the same sign, reflecting the stimulated emission from the excited states (58). If all Chls were excited with equal probabilities we would expect only one bleaching band, centered around 685 nm. This is not the case. Since the  $P700^+$  signal at the end of the reaction sequence (Figs. 4 and 5) is not larger than the 700 nm bleaching band at  $t = 0$  (Fig. 6) we can exclude the formation of a substantial amount of  $P700^+$  as the main origin of the 700-nm bleaching band at  $t = 0$ . This interpretation is also supported by the fact that the shape of the 700 nm band at  $t = 0$  is quite different from that of  $P700^+$  (DADS of  $\tau_3$ ),

TABLE 4 Wavelengths of maximal absorption bleaching and estimated absorption and fluorescence maxima for the three different Chl pigment pools (cf, Figs. 5 and 6) as deduced from transient absorption and kinetic fluorescence data

Pool	Transient absorption maximum*	Estimated absorption maximum	Estimated fluorescence maximum	Pool size, Chls
	nm			
1	685	680	690	81
2	715	710	720	4
3†	700	695	705	15

The estimated pool sizes for a total antenna size of 100 Chls are given on the basis of the transient absorption data using Eq. 2 and assuming Boltzmann equilibrium between pools (for details see text).

\* Error  $\pm 3$  nm.

† This pool also comprises P700.

which is broader. This is seen most clearly at 710 nm where the bleaching in the P700<sup>+</sup> spectrum is  $\sim 50\%$  of the bleaching at the 700-nm peak, whereas in the  $t = 0$  difference spectrum (Fig. 6) there is only little absorption change at 710 nm. Our excitation conditions select preferentially the main pool of Chls, absorbing maximally at  $\sim 678$  nm (Fig. 1A). The fact that we observe about equally intense bleachings at 685 and 700 nm can only be accounted for if we assume that actually an energy transfer process occurs in a time shorter than the time resolution of our experiment. This ultrafast energy transfer redistributes excitons from the initially excited main antenna pool (F690, absorption bleach at 685 nm) to a pool of pigments with an absorption bleach close to 700 nm. That process must have a lifetime shorter than 3 ps, the time resolution of our experiment, and leads to a kind of (transient) equilibrium state between pigments with absorption bleachings at 685 and 700 nm, respectively. This interpretation then requires a total of at least three pools of spectrally well-distinguished Chls plus P700, i.e., the pools with absorption bleaches at 685 nm (pool 1), 715 nm (pool 2), and 700 nm (pool 3) as given in Table 4, which compiles the difference absorption and the estimated absorption and fluorescence maxima of the different pools seen in transient absorption. Energy transfer components in the lifetime range of a few picoseconds have been found already earlier by transient absorption in PS I core particles from spinach (38) and the fast unresolved process in our particles might have the same origin. However, since no absorption difference spectra were presented in that work a detailed comparison with our data is difficult.

The fastest lifetimes resolved from the transient absorption ( $\tau_1 = 7-9$  ps) and from fluorescence ( $\tau_2 = 12$  ps) are quite similar. This might suggest at least in part some common origin of these components. Comparison of the curves in Fig. 6, which represent the absorption difference spectra before and after the  $\tau_1$  process, respectively, shows that the  $\tau_1$  process decreases the bleaching

at 685 nm to  $\sim 50\%$  of that present at time  $t = 0$  and concomitantly increases the bleaching at 715 nm and also slightly at 700 nm. One can thus understand qualitatively the DADS of the  $\tau_1$  component, which shows a large positive band at long wavelength (Fig. 5). The (seemingly) large absorption increase around 710–715 nm suggested by this DADS is thus only apparent (c.f., Fig. 4E, which shows only absorption bleaching at 711 nm). It simply reflects the rise (negative amplitude) of a bleaching at that wavelength developing with the time constant  $\tau_1$ . Because of the two negative signs in the absorption difference (bleaching) and in the kinetics (rise term), the decay-associated spectrum shows an overall positive sign, but nevertheless reflects an (delayed, i.e., rising) absorption bleach. Figs. 5 and 6 suggest that the maximum of this long-wavelength bleach occurs near 715 nm. This bleaching that develops with time constant  $\tau_1$  can be interpreted in a straightforward manner as an energy transfer process depopulating mainly the short-wavelength (F690) pool and populating the long-wavelength Chl pool (F720), in full agreement with the fluorescence kinetics, which suggest the same process. Overall the exciton population in the intermediate pool (pool 3) is not very much affected by this process. After this exciton migration process no further antenna processes are seen, except for the uniform decay of the Chl\* bleachings across the whole spectrum and the development of the (P700<sup>+</sup>–P700) difference signal with a time constant of  $\tau_2 = 31-35$  ps. This finding is again consistent with the fluorescence kinetics data.

The  $\tau_2$  lifetimes in transient absorption and in fluorescence are identical within the error limits. This is not the case for the  $\tau_1$  components. There exists a small but significant difference in lifetimes between transient absorption (7–9 ps) and fluorescence ( $12 \pm 1$  ps). This difference can probably be explained by the very fast ( $< 3$  ps) unresolved equilibration process discussed above. This process is too fast to influence the fitted fluorescence lifetime  $\tau_1$  in any way. The lifetime found in fluorescence therefore should represent more closely the correct lifetime for this process ( $\sim 12$  ps). In contrast, the transient absorption, which has a better, but still insufficient time-resolution, is already influenced substantially by the very fast process. Thus the  $\tau_1 = 7-9$  ps observed in transient absorption reflects a lifetime that is probably shortened by some unresolved mixing of the very fast ( $< 3$  ps) process(es) with the proper 12-ps lifetime seen nearly undisturbed in fluorescence (we should like to note here that in reality many more than two fast lifetime components are likely to be present in these particles since we expect equilibration components between all the different Chl spectral forms; c.f., Trinkunas and Holzwarth, kinetic modeling manuscript submitted for publication). We tested this interpretation by a forced fit to the transient absorption data when two lifetimes of 3 (resolution-limited) and 12 ps were fixed instead of the free-running 7–9 ps component. In this case the absorp-



tion difference at  $t = 0$  showed only one bleaching band at 685 nm as expected (see above) and not at 700 nm. In this forced fit the 700 nm bleaching (c.f., Fig. 5,  $\tau_1$ ) then develops with the time constant of the fixed 3-ps component, whereas the other components are not substantially influenced. However, in a free-running fit these two fast components could not be separated and faster measuring techniques will be required to test this suggestion in detail in the future. Preliminary results from our laboratory (to be published) using femtosecond excitation pulses are, however, in line with this interpretation. The result of this discussion is summarized in Fig. 7 B which shows an extended kinetic scheme involving the three different Chl pools.

### Estimation of pool sizes from transient absorption

Typically the maximum in the absorption bleaching band of an excited state occurs close to the mirror symmetry point between the corresponding absorption and fluorescence spectrum (58). Thus, these mirror symmetry points can be obtained to a good approximation from the transient absorption spectra. This is convenient, because the mirror symmetry point provides the best measure for the excited state energy of a molecule. The corresponding ground state absorption and fluorescence maxima of these pigments should then be located symmetrically around the absorption bleach maximum. Applying this rationale to the DADS and using similar Stokes shifts for all Chl pools ( $\sim 10$  nm) we get the data summarized in Table 3.

We are particularly interested to derive the relative pool sizes of the three antenna pools. From the absorption difference spectra we can in fact obtain a rough estimate of the sizes of the various Chl pools. As discussed above, pools 1 and 3 seem to equilibrate in a time shorter than the time resolution of the transient absorption. Thus the bleaching at  $t = 0$  essentially should reflect the situation after that equilibration has already occurred. In view of the lack of other information, we assume identical absorption difference coefficients for all Chls, which is probably quite a reasonable approximation. The relative bleachings at 685 and at 700 nm then provide a direct measure of the relative exciton density in the pools 1 and 3, which is identical to the equilibrium constant  $K_{eq}$  for the excitons in these pools. Applying equilibrium thermodynamics we can thus calculate relative antenna sizes  $N_i/N_j$  using the Boltzmann equation and its relationship to rate constants:

$$\frac{k_{ji}}{k_{ij}} = K_{eq} = \frac{N_i}{N_j} \times \exp^{-(E_i - E_j)/k_B T}, \quad (2)$$

where  $k_{ij}$  is the overall rate constant of energy transfer from pool  $j$  to pool  $i$ ,  $N_i$  is the pool size (number of Chls),  $E_i$  the excited state energy, and  $k_B$  the Boltzmann constant.  $K_{eq}$  is obtained directly from the ratio in the

bleaching amplitudes ( $\Delta A(\lambda_d)$ ) of the pools at their respective bleaching maxima in Fig. 6 (for an exact determination a spectral decomposition would be required in addition but the error is reasonably small here since the bands do not overlap strongly). Thus the relative pool sizes of pools 1 and 3 can be estimated, assuming that equilibration with other pools will be significantly slower, as seems to be the case. Likewise the equilibrium constant between pools 3 and 2 can be obtained from the absorption difference spectrum  $\Sigma_{2+3}$  (Fig. 6). From the about equal bleaching at 700 and 715 nm (Fig. 6) it follows that the absorption bleach in pools 2 and 3 is about equal in the equilibrium state. The results of these estimates, which provide the ratios of the Chls in the different pools, are summarized in Table 4. Normalizing for a total antenna size of 100 Chls, this implies that the particles studied here should contain  $\sim 4 \pm 1$  long-wavelength Chls (pool 2, F720). It is not known where these long-wavelength Chls are located in the PS I complex. However, taking into account results from recent simulations of energy transfer in model Chl arrays (23, 35) it is most likely that the long-wavelength Chls are situated somewhere close to the RC or at least are connected by a special channel with the RC. Further details on their position could be revealed by more specific simulations. If our conclusion about the location of the long-wave Chls is correct, the RC P700\* state should probably be in close contact with the F720-nm-emitting pigments.

### SAS and SADS

The data discussed so far suggest that the P700\* shows similar kinetics as and is in equilibrium with the long-wavelength Chl forms. This further suggests that the RC is located near these long-wavelength pigments in the antenna. In a simple compartmental model then P700 could be made part of the long-wavelength pool. However, the alternative situation that P700 is spatially and kinetically more closely related to the short-wavelength pool can not be excluded a priori. We have tested by target analysis both of these two different kinetic models as shown in Fig. 7, A and C. The difference between these models consists in the assumed location and coupling of the reaction center P700. The model in Fig. 7 A assumes P700 to be located within, and thermally equilibrated with, the pigments of the long-wavelength pool 2 (F720). In contrast, the model in Fig. 7 C assumes that the RC is located within, and equilibrated with, the short-wavelength pool 1 (F690). The rate constants resulting from this analysis are given in Tables 2 and 3. The SAS for fluorescence and the SADS for transient absorption for both models are shown in Fig. 8.

The two models give quite different results in terms of rate constants (c.f., Table 2 and 3) and also in terms of the SAS and SADS (Fig. 8). Comparing first the rate constants for the two models one notices that in both transient absorption and fluorescence data qualitatively similar differences between the two models are observed:

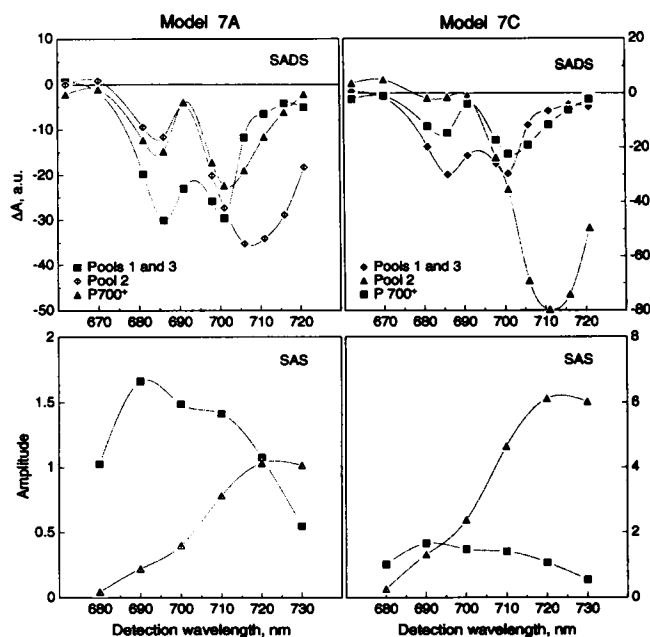


FIGURE 8 Species-associated difference absorption spectra (SADS) (top) and fluorescence SAS (bottom) of the two different kinetic models shown in Fig. 7 A (left) and C (right), as calculated by target analysis.

for the model in Fig. 7 A the forward rate for energy transfer from pool 1 to pool 2 ( $k_{21}$ ) is several times faster than the reverse rate ( $k_{12}$ ). This is expected from simple thermodynamic considerations since pool 2 is located at lower energy. This energetic factor can also not be compensated completely by the entropic term, i.e., the fact that pool 2 contains fewer pigments than pool 1. Thus for energetic reasons a ratio of *apparent transfer* rate constants  $k_{21}/k_{12} > 1$  is required. The same conclusion follows already from the steady state fluorescence spectra, which show that the exciton equilibrium is on the side of the F720 pool. This requirement is fulfilled only for the model in Fig. 7 A but not for the model in Fig. 7 C. This fact alone is already sufficient to exclude the model in Fig. 7 C as a physically reasonable interpretation of the data. However, the SAS and the SADS (Fig. 8) provide additional arguments for excluding the model in Fig. 7 C. The SAS and SADS represent the pure fluorescence and difference absorption spectra, respectively, for the intermediates involved. Thus we expect the SADS to represent the (Chl\*–Chl) difference spectra of Chl pools 1 and 2 and in addition the (P700<sup>+</sup>–P700) difference spectrum. Assuming similar difference extinction coefficients for all Chls involved we would expect SADS of similar maximal bleaching amplitude for all excited Chl pools. This expectation is fulfilled quite well for the model in Fig. 7 A. Also the bleaching maxima occur in the expected wavelength ranges. Furthermore the calculated (P700<sup>+</sup>–P700) spectrum in this case is very close to the well-known published (P700<sup>+</sup>–P700) spectra. In contrast, the SADS for the model in Fig. 7 C look quite

odd according to these criteria. First, the difference spectrum of pool 2 is unexpectedly large as compared with that of pool 1. Furthermore, the predicted (P700<sup>+</sup>–P700) spectrum in this case deviates from literature data in the long wavelength range. Similar results are obtained in the SAS from fluorescence. The two SASs for the model in Fig. 7 C have largely different amplitudes and also largely different areas under the curves (The area under a SAS is proportional to the radiative rate). This would imply largely different radiative rates for the two Chl pools, which is quite unlikely. In contrast for the model in Fig. 7 A we estimate quite similar radiative rates from the SAS and thus a much better agreement with expectations. We thus can exclude the model in Fig. 7 C also on the basis of the species-associated spectra. Although the model in Fig. 7 C fits the data formally well it leads to physically unreasonable results and must be discarded. We can thus conclude that the long-wavelength pigments should be in close association with the RC. One should be aware of the fact however that this represents only a *minimal kinetic model* and refinement will be necessary, in particular by incorporating more Chl pools, as more kinetic data become available. More details of the Chl organization could be revealed also by exact kinetic simulations. We should like to note here that the model in Fig. 7 C was actually proposed as a suitable kinetic model for PS I in reference 34.

### Comparison with kinetic data on other core PS I particles

At this point a comparison with kinetic measurements on cyanobacterial or other core PS I particles is of interest. We do not include large PS I particles in this comparison, because their kinetics is substantially different. Wittmershaus et al. (34) also reported a very fast decay component of 14 ps in a PS I particle from *Phormidium*, which was of similar size as ours. They analyzed their decays in terms of a biexponential model with the second lifetime being as long as 84 ps. Thus, assuming a small amount of (unresolved) longer-lived components in their preparation, their kinetics may be very similar to ours. However, since they did not wavelength resolve the fluorescence but observed the integral emission, they most likely missed the rising part of the shortest-lived component at long wavelengths. This led them to explain their data in terms of a model that is at variance with our data. They attributed the fast component to the trapping of the excitons from the core antennae by the reaction center P700. Their longer-lived component was attributed to the trapping of the excitons from the peripheral antenna (34). We can exclude this possibility for the particles studied here on the grounds discussed above in detail (see discussion of SAS and SADS above). Provided that singlet annihilation can be excluded in their data, an indication for a rapid energy transfer component may have been observed in transient absorption experiments also in reference 33.

Our model in Fig. 7 C shows qualitative similarities to a model proposed by Wittmershaus (12). Although there are substantial differences in the exact values of rate constants between their data set and ours, we agree with the conclusion of Wittmershaus, that our intermediate pool 3 (corresponding to C697 in reference 12) serves as an intermediate trap for excitations reaching P700. We can not exclude at present that this fact could lead to a fast rising contribution in the P700<sup>+</sup> kinetics in addition to the 35-ps component. Such a hypothetical fast component should not have a very large relative amplitude, however (see above), but this point needs to be clarified in further experiments on a faster time scale. Although the Chl spectral composition may be somewhat different in core PS I particles from higher plants, very similar lifetimes as reported here were observed by transient absorption in PS I core particles from spinach (38). In addition, components of 1–3 ps whose presence is also suggested indirectly by our time-resolved spectra (but remained unresolved in our data because of insufficient time resolution) were resolved in that study. However, since no transient absorption spectra were measured in that study (38), an assignment and comparison of their data and ours is not easily possible. Klug et al. (58) measured very small particles with an antenna-size of 31 Chls. A fast red-shift (within  $\approx 3$  ps) of the initial transient absorption can be seen in their transient spectra as well. However, their data do not show evidence for the presence of a long-wavelength pool (F720). This difference is very interesting because it might be diagnostic with respect to the location of the F720 pigments in the different core PS I antenna.

### Trap- versus diffusion-limited kinetics

It is fundamental for understanding the exciton kinetics in an antenna/RC complex whether the overall decay kinetics of the excited state is limited by energy transfer (diffusion limited case) or by the trapping process (charge separation in the RC) itself and is thus called trap limited (3, 7, 8, 59). These two cases represent the extremes and in principle each intermediate situation is possible in reality as well. Our data show clearly that the equilibration over the majority of the antenna Chls, i.e., all those Chl pools absorbing below 700 nm, is complete in a time  $< 3$  ps (still unresolved in our measurements). Only the few long-wavelength Chls responsible for F720 and F735 and perhaps a few of the  $\sim 700$ -nm-absorbing Chls equilibrate more slowly with the bulk antenna, i.e., with a time constant of 12 ps. Our data show that after that time the antenna is essentially equilibrated, i.e., the 12-ps component represents the slowest energy transfer time in the system. This follows both from the kinetics in transient absorption and from the fluorescence kinetic data. We thus conclude that most energy transfer processes occur in a time scale 10 times faster than charge separation and that equilibration with a small pool of long-wavelength pigments still occurs on a time scale

three times faster than charge separation. If we make the reasonable assumption that the red pigments are situated near the RC (23, 25) then the  $\tau_1 = 12$ -ps component would be more or less also representative of the time-limiting energy transfer process from the bulk antenna to the RC, although we can not exclude at present an additional and faster direct transfer path to the RC, circumventing the long-wavelength pigments. All these observations then sum up to the conclusion that the overall kinetics in the core antenna of PS I is essentially trap-limited, although the slowest energy transfer and the charge separation differ by less than an order of magnitude in time scale. This conclusion is in some discrepancy with previous conclusions of Owens et al. (6, 14) that the exciton kinetics in PS I should be nearly diffusion limited. The most reasonable explanation for this discrepancy in interpretations might consist in the fact that Owens et al. based their interpretation on data where the fast (equilibration)  $\tau_1$  component was not resolved.

### Is there evidence for electron acceptor A<sub>0</sub> in our data?

A Chl molecule has been suggested as the primary electron acceptor in PS I RCs, on the basis of low temperature EPR spectra (45, 60) and transient absorption data. (43, 47, 61). Our transient absorption data do not indicate any processes slower than  $\sim 40$  ps that would occur on the time scale up to several nanoseconds and causing absorption changes in the visible range. After formation of P700<sup>+</sup> with  $\approx 35$  ps lifetime, no further absorption changes occur in the wavelength range examined, which should comprise all possible Chls. Thus our results are only consistent with one of the following possibilities: (a) The reduction of the primary acceptor A<sub>0</sub> does not cause an absorption change in the visible. This would exclude, inter alia, also a Chl pigment as the primary acceptor. (b) Electron transfer could occur directly to A<sub>1</sub>, which is believed to be a quinone (vitamin K<sub>1</sub>) (62), or to another, so far unknown acceptor. This possibility cannot be excluded. A further possibility exists: (c) The reoxidation of a Chl anion close to P700 would be expected to be coupled at least with an electrochromic shift, either in the P700<sup>+</sup> band itself or in some surrounding Chl. Since no such corresponding spectral or kinetic component is observed it implies that no electron transfer steps occur between  $\sim 40$  ps and several nanoseconds after the pulse. We can thus conclude that if there exists an acceptor preceding A<sub>1</sub>, reoxidation of its reduced form must occur either on a time scale faster than 40 ps or much slower than several nanoseconds. The latter case can be excluded from measurements on slower time scales (43). If the first case applies, i.e., reoxidation of A<sub>0</sub><sup>-</sup> faster than its formation, the intermediate would be difficult, if not impossible, to detect because its maximal transient concentration would be very small at all times. This conclusion has been reached by Nuijs et

al. (47) and Shuvalov et al. (43). Our data are consistent with this possibility. However, so far unequivocal direct evidence for the existence and identity of  $A_0$  is still scarce. The transient absorption data reported earlier in favour of the  $A_0^-$  intermediate being a Chl anion (47) look very unusual, given the absorption difference signal, which shows sharp features around 680 and 700 nm. A more convincing difference spectrum for a Chl anion was produced later by Shuvalov et al. (43), however, only when secondary acceptors were reduced. The conclusions drawn in that paper are valid only if one assumes, as implied by the authors, that one can exclude any effects on the nature or rate of the primary electron transfer process upon reduction of secondary acceptors. We should like to note that, e.g., in PS II, reduction of the secondary acceptor  $Q_A$  has dramatic effects on the primary charge separation rate (8, 31, 54). In summary, given the limitations discussed above, on the one hand our data are not inconsistent with the idea of a Chl being the primary electron acceptor in PS I, provided it is reoxidized in <40 ps. On the other hand, they also do not provide any evidence in favor of this hypothesis. The case of the electron going directly to  $A_1$  cannot be excluded either. To further clarify this point it would be clearly desirable and more convincing to detect the kinetics of  $A_0$  directly in centers without reduced secondary acceptors. This experiment has been carried out by Shuvalov et al. (43), albeit with fairly long excitation pulses.

## Conclusion

Despite the seemingly unusual steady state and time-resolved fluorescence spectra of this preparation studied here, comparison of our kinetics and spectra in this cyanobacterial PS I system with a PS I core preparation from spinach of roughly similar antenna size indicates that neither the spectra and kinetics nor the content of red pigments in this cyanobacterial PS I core is unusual. The similarity with the spinach data is in fact quite pronounced (55) and is furthermore in line with the general view that core antenna of higher plants and cyanobacteria have very similar structure and composition (2). The fact that the steady state fluorescence in this preparation is peaking near 720 nm is simply due to the fact that the amount of functionally uncoupled Chl is extremely low in our preparation. These uncoupled Chl pigments are generally responsible for the blue-shifted fluorescence (emission maximum in the range 670–685) in most PS I preparations (64) as can be concluded clearly also from the time-resolved spectra where the possible contribution from decoupled Chl can be exactly accounted for (1, 30).

It is thus interesting to compare our data with those of Owens et al. (6, 14) and Werst et al. (35). No rise terms, neither at room temperature nor at low temperature, have been resolved in their studies. Werst et al. studying PS I particles from *Chlamydomonas* of ~40–50 Chls/

P700 (core antenna) and 120–130 (Chl a+b/P700) got quite different results as compared with ours. Already their steady state spectra look quite different from ours, i.e., they show very little red (F720) fluorescence, which may indicate a substantially lower content of red Chls in their preparations. This also holds for the earlier data of Owens et al. (6, 14). We conclude that the spectra as well as the kinetics of the PS I particles studied by Owens et al. and Werst et al. are of the more unusual type with respect to the low content of red pigments and the shape of the fluorescence spectra. First, they do not show the strong F720 fluorescence band as this cyanobacterial PS I and also the PS I from spinach (54, 55). Furthermore, the lifetimes found in their case do not fall on a common line with our data if one assumes a linear relationship between charge separation time and antenna size. The dependence of Owens et al. (64) would predict lifetimes about a factor of 2 longer than the experimental ones found in our case for particles of an antenna size of 100 Chls. The reason for this discrepancy remains to be clarified in the future. We should like to note, however, that a linear antenna size/lifetime relationship is not generally expected even in the trap-limited case. The overall lifetime will not only be influenced by the antenna size but also to a large extent by the content of red pigments. This factor has not been considered when deriving the linear antenna size/lifetime relationship (64) but is expected to play a decisive role.

Finally we would like to remark on the general function of red pigments. In a trap-limited system any pigments with absorption at lower energy than the RC will inevitably, and quite independent of the antenna structure, lead to a lengthening of the charge separation time (see Trissl and Holzwarth, manuscript submitted for publication). Thus such red pigments cannot increase but do rather decrease the efficiency of charge separation, quite in contrast to the hypothesis put forward in the literature (18, 19). If these red pigments are located near the RC they would definitely concentrate the excitons near the RC as suggested (19). However, this has no beneficial effect on the rate nor on the efficiency of charge separation. These conclusions are of general nature for all trap-limited systems. Why nature chose to add red pigments thus is not obvious at all. One should note, however, that even with the red pigments present, in this core PS I preparation, the charge separation is ~100 times faster than the antenna Chl decay and charge separation efficiency will thus be >95%, ignoring any other possible deactivation processes. Under these conditions the presence of red pigments does not significantly lower the efficiency and PS I can "afford" such unfavorable pigments easily.

We thank U. Pieper for preparing the PS I particles and Mrs. A. Keil for technical support during the measurements. We also thank Prof. K. Schaffner for his interest and support of this work.

Partial financial support by the Deutsche Forschungsgemeinschaft (Projekt HO-924/1-3 und Sonderforschungsbereich 189, Heinrich-

Received for publication 4 November 1992 and in final form 8 February 1993.

## REFERENCES

- Holzwarth, A. R., W. Haehnel, R. Ratajczak, E. Bittersmann, and G. H. Schatz. 1990. Energy transfer kinetics in photosystem I particles isolated from *Synechococcus* sp. and from higher plants. In *Current Research in Photosynthesis*. M. Baltscheffsky, editor. Kluwer Academic Publishers, Dordrecht, The Netherlands. 611–614.
- Golbeck, J. H., and D. A. Bryant. 1991. Photosystem-I. *Curr. Top. Bioenerg.* 16:83–177.
- Holzwarth, A. R. 1991. Excited-state kinetics in chlorophyll systems and its relationship to the functional organization of the photosystems. In *Chlorophylls*. H. Scheer, editor. CRC Press, Boca Raton, FL. 1125–1151.
- Holzwarth, A. R. 1989. Applications of ultrafast laser spectroscopy for the study of biological systems. *Q. Rev. Biophys.* 22:239–326.
- McCauley, S. W., E. Bittersmann, and A. R. Holzwarth. 1989. Time-resolved ultrafast blue-shifted fluorescence from pea chloroplasts. *FEBS (Fed. Eur. Biochem. Soc.) Lett.* 249:285–288.
- Owens, T. G., S. P. Webb, L. Mets, R. S. Alberty, and G. R. Fleming. 1987. Antenna size dependence of fluorescence decay in the core antenna of photosystem I: estimates of charge separation and energy transfer rates. *Proc. Natl. Acad. Sci. USA* 84:1532–1536.
- van Grondelle, R. 1985. Excitation energy transfer, trapping and annihilation in photosynthetic systems. *Biochim. Biophys. Acta* 811:147–195.
- Holzwarth, A. R., and T. A. Roelofs. 1992. Recent advances in the understanding of chlorophyll excited state dynamics in thylakoid membranes and isolated reaction centre complexes. *J. Photochem. Photobiol. B Biol.* 15:45–62.
- Boekema, E. J., J. P. Dekker, M. G. van Heel, M. Rögner, W. Saenger, I. Witt, and H. T. Witt. 1987. Evidence for a trimeric organization of the photosystem I complex from the thermophilic cyanobacterium *Synechococcus* sp. *FEBS (Fed. Eur. Biochem. Soc.) Lett.* 217:283–286.
- Witt, I., H. T. Witt, D. Di Fiore, M. Rögner, W. Hinrichs, W. Saenger, J. Granzin, C. Betzel, and Z. Dauter. 1988. X-ray characterization of single crystals of the reaction center I of water splitting photosynthesis. *Ber. Bunsen-Ges. Phys. Chem.* 92:1503–1506.
- Kühlbrandt, W., and D. N. Wang. 1991. Three-dimensional structure of plant light-harvesting complex determined by electron crystallography. *Nature (Lond.)* 350:130–134.
- Wittmershaus, B. P. 1987. Measurements and kinetic modeling of picosecond time-resolved fluorescence from photosystem I and chloroplasts. In *Progress in Photosynthesis Research*. J. Biggins, editor. Nijhoff Publishers, Dordrecht, The Netherlands. 75–82.
- Shiozawa, J. A., R. S. Alberty, and J. P. Thornber. 1974. The P<sub>700</sub>-chlorophyll a-protein. Isolation and some characteristics of the complex in higher plants. *Arch. Biochem. Biophys.* 165:388–397.
- Owens, T. G., S. P. Webb, R. S. Alberty, L. Mets, and G. R. Fleming. 1988. Antenna structure and excitation dynamics in photosystem I. I. Studies of detergent-isolated photosystem I preparations using time-resolved fluorescence analysis. *Biophys. J.* 53:733–745.
- Friedrich, J., and D. Haarer. 1984. Photochemical hole-burning and optical relaxation spectroscopy in polymers and glasses. *Angew. Chem.* 96:96–123.
- Gillie, J. K., G. J. Small, and J. H. Golbeck. 1989. Nonphotochemical hole burning of the native antenna complex of photosystem I (PSI-200). *J. Phys. Chem.* 93:1620–1627.
- Butler, W. L., and K. H. Norris. 1963. Lifetime of the long-wavelength chlorophyll fluorescence. *Biochim. Biophys. Acta* 66:72–77.
- Mukerji, I., and K. Sauer. 1989. Temperature-dependent steady-state and picosecond kinetic fluorescence measurements of a photosystem I preparation from spinach. In *Photosynthesis*. W. R. Briggs, editor. Alan R. Liss, New York. 105–122.
- van Grondelle, R., and V. Sundström. 1988. Excitation energy transfer in photosynthesis. In *Photosynthetic Light-Harvesting Systems*. H. Scheer and S. Schneider, editors. de Gruyter, Berlin. 403–438.
- Wendler, J., and A. R. Holzwarth. 1987. State transitions in the green alga *Scenedesmus obliquus* probed by time-resolved chlorophyll fluorescence spectroscopy and global data analysis. *Biophys. J.* 52:717–728.
- Hucke, M., Schweitzer, G., Holzwarth, A. R., Sidler, W., and Zuber, H. 1993. Studies on chromophore coupling in isolated phycobiliproteins. IV. Femtosecond transient absorption study of ultrafast excited state dynamics in trimeric phycoerythrocyanin complexes. *Biophys. J.* In press.
- Ameloot, M., J. M. Beechem, and L. Brand. 1986. Compartmental modeling of excited-state reactions: identifiability of the rate constants from fluorescence decay surfaces. *Chem. Phys. Lett.* 129:211–219.
- Beauregard, M., I. Martin, and A. R. Holzwarth. 1991. Kinetic modelling of exciton migration in photosynthetic systems. (1) Effects of pigment heterogeneity and antenna topography on exciton kinetics and charge separation yields. *Biochim. Biophys. Acta* 1060:271–283.
- Jean, J. M., C.-K. Chan, G. R. Fleming, and T. G. Owens. 1989. Excitation transport and trapping on spectrally disordered lattices. *Biophys. J.* 56:1203–1215.
- Jia, Y., J. M. Jean, M. M. Werst, Ch. Chan, and G. R. Fleming. 1992. Simulations of the temperature dependence of energy transfer in the PS I core antenna. *Biophys. J.* 63:259–273.
- Suter, G. W., and A. R. Holzwarth. 1987. A kinetic model for the energy transfer in phycobilisomes. *Biophys. J.* 52:673–683.
- Campillo, A. J., S. L. Shapiro, N. E. Geacintov, and C. E. Swenberg. 1977. Single-pulse picosecond determination of 735 nm fluorescence risetime in spinach chloroplasts. *FEBS (Fed. Eur. Biochem. Soc.) Lett.* 83:316–320.
- Pellegrino, F., A. Dagen, P. Sekuler, and R. R. Alfano. 1983. Temperature dependence of the 735 nm fluorescence kinetics from spinach measured by picosecond laser-streak camera system. *Photobiophys. Photobiophys.* 6:15–23.
- Searle, G. F. W., R. Tamkivi, A. van Hoek, and T. J. Schaafsma. 1988. Temperature dependence of antenna chlorophyll fluorescence kinetics in photosystem I reaction center protein. *J. Chem. Soc. Faraday Trans. II* 84:315–327.
- Turconi, S., G. Schweitzer, and A. R. Holzwarth. 1993. Temperature dependence of picosecond fluorescence kinetics of a cyanobacterial photosystem I particle. *Photochem. Photobiol.* 57:113–119.
- Schatz, G. H., H. Brock, and A. R. Holzwarth. 1988. A kinetic and energetic model for the primary processes in photosystem II. *Biophys. J.* 54:397–405.

32. Holzwarth, A. R., W. Haehnel, J. Wendler, G. W. Suter, and R. Ratajczak. 1984. Picosecond fluorescence kinetics and energy transfer in antennae chlorophylls of green algae and membrane fractions of thylakoids. In *Advances in Photosynthesis Research*. C. Sybesma, editor. Nijhoff Publishers, The Hague. 73–76.
33. Evans, E. H., R. Sparrow, and R. G. Brown. 1987. Fast fluorescence and absorption measurements of photosystem I from a cyanobacterium. In *Progress in Photosynthesis Research*. J. Biggins, editor. Nijhoff, Dordrecht, The Netherlands. 99–102.
34. Wittmershaus, B. P., D. S. Berns, and C. Huang. 1987. Picosecond time-resolved fluorescence from detergent-free photosystem I particles. *Biophys. J.* 52:829–836.
35. Werst, M., Y. W. Jia, L. Mets, and G. R. Fleming. 1992. Energy transfer and trapping in the photosystem I core antenna. A temperature study. *Biophys. J.* 61:868–878.
36. Causgrove, T. P., S. Yang, and W. S. Struve. 1989. Polarized pump-probe spectroscopy of photosystem I antenna excitation transport. *J. Phys. Chem.* 93:6844–6850.
37. Lyle, P. A., and W. S. Struve. 1991. Temperature dependence of antenna excitation transport in native photosystem-I particles. *J. Phys. Chem.* 95:4152–4158.
38. Causgrove, T. P., S. M. Yang, and W. S. Struve. 1988. Electronic excitation transport in core antennae of enriched photosystem I particles from spinach chloroplasts. *J. Phys. Chem.* 92:6121–6124.
39. Pashchenko, V. Z., L. A. Avramov, S. Vasil'ev, V. V. Gorokhov, B. N. Korvatovskii, G. P. Kukarskikh, and A. B. Rubin. 1986. Picosecond spectroscopy of charge separation and recombination processes in reaction centers of photosystem I in higher plants. *Mol. Biol.* 20:755–764.
40. Klug, D. R., L. B. Giorgi, B. Crystall, J. Barber, and G. Porter. 1989. Energy transfer to low energy chlorophyll species prior to trapping by  $P_{700}$  and subsequent electron transfer. *Photosynth. Res.* 22:277–284.
41. Shuvalov, V. A., A. V. Klevanik, A. V. Sharkov, P. G. Kryukov, and B. Ke. 1979. Picosecond spectroscopy of photosystem I reaction centers. *FEBS (Fed. Eur. Biochem. Soc.) Lett.* 107:313–316.
42. Mansfield, R. W., and M. C. W. Evans. 1985. Optical difference spectrum of the electron acceptor AO in photosystem I. *FEBS (Fed. Eur. Biochem. Soc.) Lett.* 190:237–241.
43. Shuvalov, V. A., A. M. Nuijs, H. J. van Gorkom, H. W. J. Smit, and L. N. M. Duysens. 1986. Picosecond absorbance changes upon selective excitation of the primary electron donor P-700 in photosystem I. *Biochim. Biophys. Acta.* 850:319–323.
44. Mansfield, R. W., and M. C. W. Evans. 1986. Primary acceptors in photosystem I. *Biochem. Soc. Trans.* 14:49–50.
45. Bonnerjea, J., and M. C. W. Evans. 1982. Identification of multiple components in the intermediary electron carrier complex of photosystem I. *FEBS (Fed. Eur. Biochem. Soc.) Lett.* 148:313–316.
46. Smith, N. S., R. W. Mansfield, J. H. A. Nugent, and M. C. W. Evans. 1987. Characterization of electron acceptors  $A_0$  and  $A_1$  in cyanobacterial photosystem I. *Biochim. Biophys. Acta.* 892:331–334.
47. Nuijs, A. M., V. A. Shuvalov, H. J. Van Gorkom, J. J. Plijter, and L. N. M. Duysens. 1986. Picosecond absorbance difference spectroscopy on the primary reactions and the antenna-excited states in photosystem I particles. *Biochim. Biophys. Acta.* 850:310–318.
48. Miyairi, S., and G. H. Schatz. 1983. Oxygen-evolving extracts from a thermophilic cyanobacterium *Synechococcus sp. Z. Naturforsch. Sect. C Biosci.* 38:44–48.
49. Markwell, J. P., J. P. Thornber, and M. P. Skrdla. 1980. Effect of detergents on the reliability of a chemical assay for P-700. *Biochim. Biophys. Acta.* 591:391–399.
50. Holzwarth, A. R., H. Lehner, S. E. Braslavsky, and K. Schaffner. 1978. Phytochrome models II: the fluorescence of biliverdin dimethyl ester. *Liebigs Ann. Chem.* 1978:2002–2017.
51. Holzwarth, A. R., J. Wendler, and G. W. Suter. 1987. Studies on chromophore coupling in isolated phycobiliproteins. II. Picosecond energy transfer kinetics and time-resolved fluorescence spectra of C-phycocyanin from *Synechococcus* 6301 as a function of the aggregation state. *Biophys. J.* 51:1–12.
52. Schatz, G. H., H. Brock, and A. R. Holzwarth. 1987. Picosecond kinetics of fluorescence and absorbance changes in photosystem II particles excited at low photon density. *Proc. Natl. Acad. Sci. USA.* 84:8414–8418.
53. Beechem, J. M., M. Ameloot, and L. Brand. 1985. Global and target analysis of complex decay phenomena. *Anal. Instrum.* 14:379–402.
54. Roelofs, T. A., C.-H. Lee, and A. R. Holzwarth. 1992. Global target analysis of picosecond chlorophyll fluorescence kinetics from pea chloroplasts. A new approach to the characterization of the primary processes in photosystem II alpha- and beta-units. *Biophys. J.* 61:1147–1163.
55. Turconi, S., N. Weber, G. Schweitzer, H. Strotmann, and A. R. Holzwarth. 1992. Energy transfer and charge separation kinetics in photosystem I. 2. Picosecond fluorescence study of various PSI particles and light-harvesting complex isolated from higher plants. *Biochim. Biophys. Acta.* In press.
56. McCauley, S. W., Bittersmann, E., and Holzwarth, A. R. 1989. Time-resolved ultrafast blue-shifted fluorescence from pea chloroplasts. *FEBS Lett.* 249:285–288.
57. Il'ina, M. D., V. V. Krasauskas, R. J. Rotomskis, and A. Y. Borisov. 1984. Difference picosecond spectroscopy of pigment-protein complexes of photosystem I from higher plants. *Biochim. Biophys. Acta.* 767:501–506.
58. Klug, D. R., B. L. Gore, L. B. Giorgi, and G. Porter. 1987. Spectral shifts in picosecond transient absorption spectra due to stimulated emission from chlorophyll in vitro and in protein complexes. In *Progress in Photosynthesis Research*. J. Biggins, editor. Nijhoff, Dordrecht, The Netherlands. 95–98.
59. Knox, R. S. 1986. Trapping events in light-harvesting assemblies. Theory and modeling of excitation delocalization and trapping. In *Encyclopedia of Plant Physiology: Photosynthesis III*, L. A. Staehelin and C. J. Arntzen, editors. Springer, Berlin. 286–298.
60. Mansfield, R. W., J. A. M. Hubbard, J. H. A. Nugent, and M. C. W. Evans. 1987. Extraction of electron acceptor  $A_1$  from pea photosystem I. *FEBS (Fed. Eur. Biochem. Soc.) Lett.* 220:74–78.
61. Shuvalov, V. A., E. Dolan, and B. Ke. 1979. Spectral and kinetic evidence for two early electron acceptors in photosystem I. *Proc. Natl. Acad. Sci. USA.* 76:770–773.
62. Brettel, K., P. Setif, and P. Mathis. 1986. Flash-induced absorption changes in photosystem I at low temperature: evidence that the electron acceptor  $A_1$  is vitamin  $K_1$ . *FEBS (Fed. Eur. Biochem. Soc.) Lett.* 203:220–224.
63. Thornber, J. P., G. F. Peter, and R. Nechushtai. 1987. Biochemical composition and structure of photosynthetic pigment proteins from higher plants. *Physiol. Plant.* 71:236–240.
64. Owens, T. G., S. P. Webb, L. Mets, R. S. Alberty, and G. R. Fleming. 1989. Antenna structure and excitation dynamics in photosystem I. II. Studies with photosynthetic mutants of *Chlamydomonas reinhardtii* lacking photosystem II. *Biophys. J.* 56:95–106.